

# The use of illitic clays in the production of stoneware tile ceramics

S. Ferrari \*, A.F. Gualtieri

*Earth Sciences Department, University of Modena and Reggio Emilia, L.go S.Eufemia 19, 41100 Modena, Italy*

Received 12 April 2005; received in revised form 7 September 2005; accepted 6 October 2005

Available online 9 November 2005

## Abstract

Illite is one of the main clay phases used for the preparation of mixtures for traditional ceramics. The raw materials used for production of white porcelain stoneware tiles mainly consist of feldspars, quartz, and clay minerals (kaolinite, smectite and illite). In this study, eight clayey raw materials with a different content of illite up to 70 wt.%, have been considered. The crystalline phases present in different amounts are illite, smectite, kaolinite, illite–smectite mixed-layers, K-feldspar, plagioclases, quartz, and accessory phases (anatase, goethite). The clays have been chemically and physically characterized as raw and fired materials with X-ray diffraction, X-ray fluorescence, and SEM. Moreover they were added in the percentage of 35 wt.% to a mixture composed of albite, feldspar sand and quartz sand, to reproduce that commonly used for the production of porcelain stoneware tiles. We focused on the quantitative mineralogical aspects of the unfired and fired bodies and their relationship with the technological properties due to the presence of illite. Increasing illite content yields higher percentage of glass phase and lower water absorption because of the lowering of the melting point. Because of the pyroplastic deformation, linear shrinkage decreases with illite content. The presence of illite inhibits the formation of mullite and cristobalite, since silica and alumina tend to form alkaline glass. Although in clays from Hungary, transition elements are present in very low percentage, the colour of the fired bodies is darker. These clays contain goethite, which may be rapidly oxidized with temperature, and show a very low percentage of newly formed mullite which could eventually host Fe in its structure.

© 2005 Elsevier B.V. All rights reserved.

*Keywords:* Illitic clays; Traditional ceramics; Firing; Glass; Ceramic tiles; Porcelain stoneware

## 1. Introduction

Knowledge of the mineralogical phase composition and especially clay fraction of the raw materials used for the preparation of ceramic mixtures is of paramount importance for understanding of the technological properties of ceramic products and optimization of firing cycles in production.

The term “illite” was first introduced by Grim et al. (1937) describing a colloidal mica-like mineral, com-

monly found in clayey sediments. Nowadays, the term “illite” refers to an aluminum–potassium mica-like, non-expanding, dioctahedral mineral, present in the clay fraction. Together with kaolinite, chlorite and smectite, illite is in fact one of the four major phases of clayey sedimentary rocks.

In accordance with the recent IMA (International Mineralogical Association) protocol on micas nomenclature (Rieder et al., 1998), dioctahedral K-micas with an interlayer cation content ranging between 0.85 and 1 per half-cell are defined muscovites, while illite forms a series with an interlayer cation content from 0.6 to 0.85. Since little is still known about the nature and stability of illite, it is not appropriate to give an ultimate

\* Corresponding author. Tel.: +39 59 205 5806; fax: +39 59 205 5887.

E-mail address: [ferrari.simone@unimore.it](mailto:ferrari.simone@unimore.it) (S. Ferrari).

definition of this phase upon a chemical basis. A more suitable term would be K-deficient mica, at least until the relationship between muscovite and illite is definitely resolved.

An approximate formula for illite, deduced by studies on natural materials (Inoue et al., 1987), can be written as (Rosenberg, 2002):  $K_{0.88}Al_2(Si_{3.12}Al_{0.88})O_{10}(OH)_2 \times nH_2O$ . An example of chemical analysis of a pure illite sample from Kaube (Japan), was given by Środoń and Eberl (1984): SiO<sub>2</sub> 47.4%, TiO<sub>2</sub> 0.23%, Al<sub>2</sub>O<sub>3</sub> 35.60%, Fe<sub>2</sub>O<sub>3</sub> 1.50%, MgO 0.30%, CaO 0.02%, Na<sub>2</sub>O 0.53%, K<sub>2</sub>O 9.12%.

Illite can be formed under several minerogenetic conditions (Środoń and Eberl, 1984). The most abundant ores were originated in weathering, diagenetic, metamorphic or hydrothermal environment, where formation mechanism is termed *illitization*. This process mainly involves the transformation of smectite into illite. Sedimentary environments may also contain illite although, because of their limited spatial distribution, they have minor importance.

There are many fields where illitic clays play an important role: illite is one of the major component of clays used in traditional ceramics for the production of cooking pots, plates, tiles and bricks. Of great importance is the application for the production of stoneware tiles, the top product in the market of traditional ceramics. Stoneware tiles present a white body whose surface may or may not be glazed, having very low water absorption and outstanding technological properties. The manufacture process basically consists of a wet milling, spray-drying, pressing, drying at 150–250 °C and firing in roller kilns (Biffi, 1997) with a  $T_{max}=1190–1230$  °C. Stoneware tiles are generally characterized by high mechanical strength, resistance to abrasion, frost and common chemical agents (acids, cleaning products, etc.). The latest trends in porcelain stoneware tile design require reformulating compositions to produce intense white color and close to zero porosity.

A recent study (Aras, 2004) reports the changes of the technological properties of mixtures with different clay composition (kaolinite-and illite-rich clay-based ceramic bodies) and shows that cristobalite formation is inhibited in illite/sericite-rich bodies. On the other hand, formation of mullite and cristobalite is observed in fired kaolinitic clays. In illite/sericite-rich mixtures, high K content produces in temperature a large amount of melt that inhibits mullite formation.

Here, we systematically studied eight clays containing different proportions of kaolinite and illite and fo-

cused the attention on the technological characteristics of the unfired and fired bodies. The first attempt is the interpretation of variations of phase composition and properties of the fired clays with respect to different content of illite in the raw material. Secondly, behavior of stoneware mixtures prepared using the eight clays has been thoroughly investigated. To this aim, we focused on the quantitative mineralogical aspects of the raw and fired bodies and relationship with the technological properties.

## 2. Materials and methods

### 2.1. Sample selection and preparation

Six clays characterized by different contents of illite and two kaolins were selected for the study. The raw materials were labeled C1 C2 C3 C4 C5 C6 C7 and C8:

- C1 kaolin from the Podborany basin (Czech Republic);
- C2 kaolin from the Troup basin (U.S.A.);
- C3 illitic clay from the Allier basin (France);
- C4 illitic clay from the Donetsk sedimentary basin (Ukraine);
- C5 and C6 illitic clays from Turkey;
- C7 and C8 illitic clays from Füzéradvány (Hungary).

Prior to the preparation of the mixtures, the eight clays were fully characterized. For each raw material a chemical, physical and mineralogical characterization was accomplished. The clays were heated up to 1200 °C, using a standard ceramic firing cycle (43') to monitor the variation of linear shrinkage and water absorption with temperature.

An ideal formulation similar to those used in the Sasuolo (Italy) district has been chosen for the preparation of the white stoneware tile mixtures. Each mixture contains 35 wt.% of one clay phase (C1 C2 C3 C4 C5 C6 C7 and C8), 40 wt.% of sodium feldspar (albite from Menderes Turkey), 15 wt.% of feldspar rich sand (from Valsugana, Italy), and 10 wt.% of quartz sand (from Florinas Sardinia, Italy). These are high quality raw material commonly used for the manufacture of stoneware tiles. The mixtures were labeled A (with C1), B (with C2), C (with C3), D (with C4), E (with C5), F (with C6), G (with C7), and H (with C8).

### 2.2. Sample characterization

Both the raw materials and the mixtures were ground using a lab wet mill (M.M.S. 1 l porcelain jar). The ground agglomerates were dried, powdered and humidified to 6 wt.%. The humid powders were pressed at 350 kg/cm<sup>2</sup> to obtain 5 cm diameter and 1 cm thick discs. Once dried, the discs were fired using a Gabbrielli (1.5 m) laboratory electric roller kiln and a 43 min long cycle

with  $T_{\max}=1180$  °C in the case of C7 and C8, and  $T_{\max}=1200$  °C for the remaining mixtures. The lower  $T_{\max}$  set for C7 and C8 is due to the fact that these clays are highly fluxing and already melted at 1200 °C. The linear shrinkage was evaluated using the formula:  $\left[\frac{L_g-L_f}{L_g}\right] \times 100$ , where  $L_g$  and  $L_f$  are the measured length of green and fired samples, respectively.

The phase composition of the powdered raw materials, green and fired products has been determined using a Philips diffractometer PW 1730 with Ni-filtered Cu  $K_{\alpha}$  radiation at 40 kV voltage and 30 mA current,  $1/2^\circ$  divergence and  $1/2^\circ$  receiving slits. Samples were collected with the side loading technique in the  $3\text{--}80^\circ$   $2\theta$  range. Data for the mineralogical quantitative analysis (QPA) of the fired products were collected in the  $10\text{--}80^\circ$   $2\theta$  range. The analysis has been performed using the Rietveld method (Young, 1993) for C1 C2 C3 C4 C5 C6. Unfortunately, the Rietveld method could not be applied to samples C7 and C8, since illite content is too high to obtain a good fit and consequently an accurate result. This is due to the lack of a structure model of disordered illite. The problem of illite has already been faced by Ferrari et al. (2005), giving a confirmation of the limits of the conventional Rietveld method with structures affected by extensive planar disorder. Semi-quantitative analyses of C7 and C8 have been derived by stoichiometric calculations. The software used for the Rietveld QPA is GSAS (Larson and Von Dreele, 1994). 10 wt.% of corundum (standard NIST 676) was used as internal standard for the determination of the amorphous phase in the fired products.

Chemical analyses were determined with an XRF spectrometer ARL 9400. The powders were heated up to 900 °C for 1 h to determine the loss of ignition as weight

difference before and after heating. 3 g of material have been mixed with organic glue; the powder support is composed of boric acid, pressed up to 8000 kg for a few min.

Stubs of specimen representative of bulk and surface of the bodies were prepared for the examination by SEM. These stubs were gold-coated (5 nm thick film). Micrographs were collected at Centro Interdipartimentale Grandi Strumenti (CIGS) of the University of Modena and Reggio Emilia using a Philips XL 40/604.

In addition, carbon, sulphur and the specific surface of the mixtures were also measured. For the determination of C and S, an infrared analyzer Eltra 900CS has been utilized.

Specific surface has been determined on the mixtures with Methylene Blue Index method (M.B.I.) (Phelps and Harris, 1967). A suspension of 10 g of mixture and 100 ml of distilled water was prepared and mixed with a methylene blue solution (10 g/l). One drop of this suspension is then placed upon filter paper and the value for the specific surface is derived from the quantity of adsorbed methylene blue.

The colour of the fired bodies has been measured and classified in terms of  $L^*$ ,  $a^*$  and  $b^*$  parameters from the CIElab system.

### 3. Results and discussion

#### 3.1. Characterization of the raw materials

The chemical and quantitative phase composition of the investigated clays are reported in Table 1. The agreement factors of the Rietveld refinements for the

Table 1  
Chemical and quantitative phase analyses of the investigated illitic clays (wt.%)

	C1	C2	C3	C4	C5	C6	C7	C8
SiO <sub>2</sub>	51.40	58.00	62.3	56.90	57.95	58.54	53.30	57.60
TiO <sub>2</sub>	0.41	1.28	1.30	1.40	1.10	1.07	0.11	0.11
Al <sub>2</sub> O <sub>3</sub>	34.50	28.00	23.00	28.30	25.90	25.43	29.40	26.30
Fe <sub>2</sub> O <sub>3</sub>	0.45	1.36	2.22	1.23	2.70	2.75	0.38	0.49
CaO	0.15	0.18	0.3	0.45	0.17	0.13	0.38	0.33
MgO	0.30	0.40	0.51	0.60	0.72	0.74	1.11	1.16
Na <sub>2</sub> O	0.15	0.26	0.28	0.59	0.25	0.24	0.28	0.26
K <sub>2</sub> O	0.58	0.54	2.01	2.25	2.47	2.67	9.31	8.47
L.O.I.	11.90	9.66	7.85	8.15	8.51	8.20	5.44	5.01
Quartz	8.9(1)	21.0(2)	33.5(2)	18.8(2)	27.2(1)	24.5(3)	21 <sup>a</sup>	27 <sup>a</sup>
Kaolinite	84.9(3)	72.0(3)	43.1(4)	37.0(4)	39.5(2)	41.6(3)	–	–
Illite	5.4(4)	5.5(4)	14.0(3)	32.9(6)	24.1(4)	27.6(5)	70 <sup>a</sup>	62 <sup>a</sup>
Smectite	–	–	1.6(4)	1.5(5)	2.5(1)	–	–	–
I–S	–	–	–	4.1(5)	–	–	7 <sup>a</sup>	6 <sup>a</sup>
K-feldspar	–	–	4.0(3)	4.2(3)	5.4(3)	4.9(3)	2 <sup>a</sup>	5 <sup>a</sup>
Anatase	0.8(2)	1.5(2)	1.3(2)	1.5(2)	1.2(1)	1.2(1)	–	–
Plagioclase	–	–	2.4(3)	–	–	–	–	–
Goethite	–	–	–	–	–	–	Traces	Traces

ESDs are reported in parentheses.

<sup>a</sup> QPA without ESDs because it was determined with stoichiometric calculation.

Table 2

Firing conditions, technological properties and quantitative phase analysis (wt.%) of the fired clays

	C1	C2	C3	C4	C5	C6	C7	C8
Temperature (°C)	1200	1200	1200	1200	1200	1200	1180	1180
Time (min)	43	43	43	43	43	43	43	43
Linear shrinkage (%)	3.59	7.29	6.97	6.89	6.74	6.70	−17.3	−15.8
Water absorption (%)	11.19	3.25	0.56	0	0	0.03	25.7	4.68
Quartz	9.6(1)	23.6(1)	23.0(1)	10.9(1)	15.1(1)	13.1(1)	1.9(2)	7.9(1)
Anatase	0.4(1)	0.4(1)	0.1(1)	0.3(6)	1.0(1)	1.0(1)	–	–
Mullite	19.8(4)	34.5(2)	27.3(2)	26.7(2)	23.6(2)	23.1(2)	5.8(3)	4.5(3)
γ-alumina	4.5(2)	–	–	–	–	–	11.9(3)	9.8(3)
Plagioclase	–	–	–	–	–	–	1.2(3)	1.2(3)
K-feldspar	–	–	2.5(2)	1.6(2)	1.3(3)	1.8(2)	2.1(3)	1.2(3)
Amorphous phase	65.7(1)	41.5(1)	47.1(2)	60.5(2)	59.0(7)	61.0(6)	77.1(1.4)	75.4(1.3)

ESDs are reported in parentheses.

QPA, as defined in GSAS (Larson and Von Dreele, 1994), were  $R_{wp}=0.11–0.14$  and  $\chi^2=1.3–1.9$ .

Regarding Ti and Fe, their amount is very different in the raw materials, and these differences will reflect variation of the tonality of the color after firing. The low content of Ti in C7 and C8 is explained by the absence of anatase or other Ti-bearing phases.

C1 and C2 contain only a small quantity of  $K_2O$ ; C3 C4 C5 and C6 contain about 2–3 wt.%  $K_2O$ ; C7 and C8 contain around 9 wt.% of  $K_2O$ . K-feldspar is always low or very low, so that  $K_2O$  is indicative of the amount of illite. As determined by Ferrari et al. (2005), about 10 wt.% of illite–smectite mixed-layers is also present. C1 and C2 have nearly the same content of illite (5.5 wt.%) but show a different kaolinite/quartz ratio. Illite content increases in C3 (14.0 wt.%), C4 (nearly 33 wt.%), C5 and C6 (24–27 wt.%). The largest content of illite is found in samples C7 and C8. Kaolinite is absent only in the Hungarian clays C7 and C8, whereas it ranges from 37 wt.% (C4) up to 84.9 wt.% (C1, which is actually a kaolin) in the other samples.

The contents of CaO, MgO and  $Na_2O$  are invariably very low (less than 0.7 wt.%) in concert with the low percentages of smectite, illite–smectite mixed-layers

and plagioclase. Na and Ca sometimes can substitute K in illite.

Table 2 resumes the firing conditions of the samples together with the linear shrinkage and water absorption of the fired bodies. Values of the linear shrinkage range from 3.59% (C1) up to 7.29% (C2) with the exception of C7 and C8 (15–17%). The dehydroxylation stage has important consequences over the stability of the fired bodies of mixtures C7 and C8, because water molecules evaporate during the dehydroxylation stage and subsequently the structure of clay minerals collapse. Since a large quantity of alkalis is present, these clays have an important fluxing action (as confirmed later) and reach the melting point at lower temperatures with respect to the other mixtures. The residual hydroxyls, eventually condensed as water molecules are kept trapped inside the body pores because early melting triggers off the formation of closed porosity, mainly at the surface of the body, which does not allow the escape of volatiles. When the sample is fired, the pressure inside the pores increases and causes deformation stress (pyroplastic deformation or expansion) upon the material. Fig. 1 reports two SEM micrographs. Image 1A shows the sample C7 fired at 1180 °C and presents coalescent

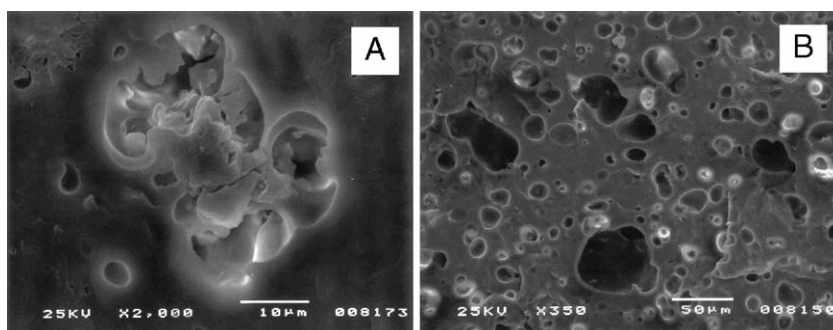


Fig. 1. SEM micrographs of sample C7 at 1180 °C (A) and sample C8 at 1220 °C (B).

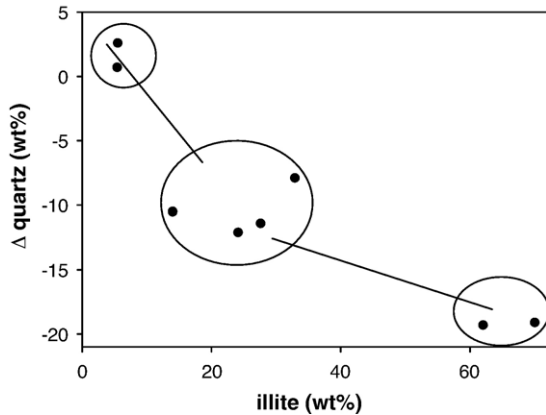


Fig. 2. Correlation between illite content (wt.%) in the raw materials and variation of quartz percentage in the firing products.

pores whose diameter is about 30–40  $\mu\text{m}$ . Image 1B represents the extreme situation of sample C8 fired at 1220  $^{\circ}\text{C}$  with linked pores larger than 50  $\mu\text{m}$ .

The water absorption is nearly zero for C4, C5 and C6, and increases for C3 (0.56%). The other samples show a larger value: C2 and C8 with about 5%, C1 with 11.19%. The highest value is found for C7 (25.7%). The reasons for the large values measured in C1 and C7 are different as there are vast differences in the mineralogical content of the two clays. The water absorption in the Hungarian clay is justified by the large pores formed according to the model previously described. On the contrary, the Czech kaolin contains pores, whose origin is linked to the refractory nature of the material. The high values measured in C2 and C8 can be explained invoking the same reasons because C2 has a large content of kaolinite, whereas C8 contains predominant illite.

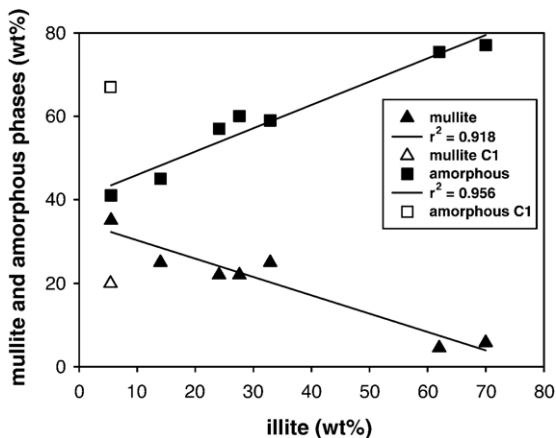


Fig. 3. Correlations between illite in the raw materials and mullite and amorphous phase in the fired clays. C1 is not considered in the calculation of the  $r^2$  coefficient.

The QPA of the fired clays is reported in Table 2. The refined weight of quartz tends to decrease with increasing the illite phase (see Fig. 2). Mullite follows the same trend of quartz (Fig. 3). Illite apparently inhibits the formation of mullite which is distinctive of kaolinitic clays. In fact, mullite directly forms from metakaolinite, the dehydroxilated product of kaolinite. Oppositely, a positive trend has been found between illite and the amorphous phase, because of the fluxing action of the interlayer cations of illite, which also inhibits the formation of cristobalite, as already stated by Aras (2004). Cristobalite has not been found in the fired products. The large content of K in the illitic clays determines the formation of an alkaline melt which is an unfavorable chemical environment for cristobalite.

Sample C1, given the content of 5.4 wt.% of illite in the unfired clay, shows a surprisingly large amount of amorphous phase. As a matter of the fact, the nature of the amorphous phase in C1 is different from that of the other clays. In fact, this amorphous phase is actually a porous aggregate of sintered particles, not a melt. On the contrary, the fluxing action of alkalis generates the glass found in the other fired samples.

Table 3

Formulation, chemical composition (wt.%) and specific surface area ( $\text{m}^2/\text{g}$ ) of the investigated ceramic mixtures

	A	B	C	D	E	F	G	H
C1	35	–	–	–	–	–	–	–
C2	–	35	–	–	–	–	–	–
C3	–	–	35	–	–	–	–	–
C4	–	–	–	35	–	–	–	–
C5	–	–	–	–	35	–	–	–
C6	–	–	–	–	–	35	–	–
C7	–	–	–	–	–	–	35	–
C8	–	–	–	–	–	–	–	35
Albite	40	40	40	40	40	40	40	40
Feldspar	15	15	15	15	15	15	15	15
sand								
Quartz	10	10	10	10	10	10	10	10
sand								
SiO <sub>2</sub>	66.90	69.40	70.70	69.5	69.20	68.10	66.50	68.10
TiO <sub>2</sub>	0.27	0.55	0.55	0.59	0.46	0.47	0.15	0.15
Al <sub>2</sub> O <sub>3</sub>	21.57	19.20	17.70	18.89	18.60	19.38	20.37	19.22
Fe <sub>2</sub> O <sub>3</sub>	0.21	0.54	0.81	0.47	1.08	1.07	0.20	0.25
CaO	0.45	0.43	0.48	0.54	0.40	0.36	0.47	0.46
MgO	0.12	0.13	0.19	0.21	0.40	0.37	0.66	0.66
Na <sub>2</sub> O	4.29	4.35	4.34	4.41	4.39	4.36	4.61	4.49
K <sub>2</sub> O	1.28	1.29	1.85	1.84	2.07	2.19	4.45	4.14
L.O.I.	4.56	3.84	3.12	3.29	3.18	3.45	2.35	2.27
CO <sub>2</sub>	n.d.	n.d.	n.d.	n.d.	n.d.	n.d.	n.d.	n.d.
C	0.03	0.05	0.05	0.03	0.078	0.063	0.026	0.025
S	n.d.	0.06	0.01	n.d.	0.019	0.014	0.003	0.011
Specific surface	32.0	34.2	34.0	43.2	36.8	36.3	48.8	46.0



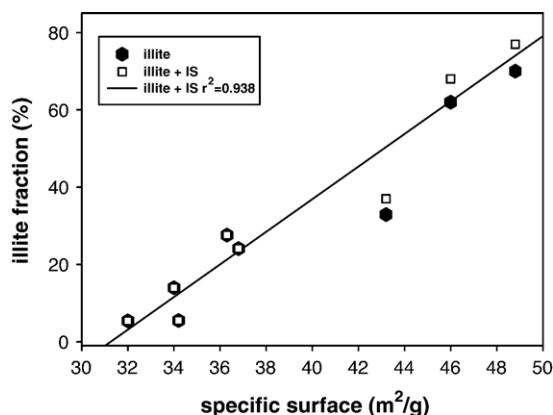


Fig. 4. Correlation between the illite (and/or illite+IS clay phases) content and the specific surface of the mixture.

### 3.2. Behaviour of illitic clays in the ceramic mixtures

The formulation of mixtures prepared to reproduce a common white stoneware tile mixture is reported in Table 3, which also contains their chemical characteristics and specific surface. When compared to the chemical analyses of Table 1, transition elements (iron and titanium) decrease, ranging between 0.35 (G) and 1.54 wt.% (E and F) and the content of K<sub>2</sub>O depends on the mixture considered. For example, A and B have values up to 1.28–1.29 wt.%, C–F have contents similar to the content of the clays, whereas the content is clearly decreased in G–H. Silica and alumina reflect the same differences revealed by the investigated clays: mixture C has the largest SiO<sub>2</sub> content and the lowest Al<sub>2</sub>O<sub>3</sub> content. On the other hand, A shows the lowest percentage of SiO<sub>2</sub> (together with G) and the largest Al<sub>2</sub>O<sub>3</sub> content.

CO<sub>2</sub> is below the detection limit for all the samples, indicating that carbonates are not present in the ceramic mixtures. Organic carbon (indicative of organic matter) ranges from a minimum of 0.025 wt.% (H) up to 0.078 wt.% (E). Such a low amount of organic matter is a positive characteristic of the ceramic mixtures as it would not cause exothermic reactions and reduced en-

vironment in the core of the bodies during firing. Similarly, the low concentration of S in all the mixtures is an indication that no volatile compounds will be released during firing.

The values of the specific surface show a large variability (from 32.0 m<sup>2</sup>/g (A) to 48.8 m<sup>2</sup>/g (G)). The largest values were measured for the mixtures G, H and D, whose predominant clay phases is illite. This is an expected result, since the specific surface of kaolinite is usually considerably smaller (10–20 m<sup>2</sup>/g) with respect to that of illite (80–100 m<sup>2</sup>/g). A linear correlation (Fig. 4) has been found between the illite (and/or illite+IS clay phases) content and the specific surface of the mixture. This is a clear indication that the overall increase of the specific surface of the body mixtures is due to the increasing weight of illite (and interlaminate illite–smectite IS).

All the mixtures were fired at different temperatures up to 1220 °C, and fully characterized. In Table 4, the results of the QPA with the Rietveld method on the samples fired at 1200 °C are shown. The agreement factors of the Rietveld refinements, as defined in GSAS (Larson and Von Dreele, 1994) were  $R_{wp}=0.070\text{--}0.093$  and  $\chi^2=1.1\text{--}1.4$ . Quartz, mullite, feldspars and amorphous phase are detected. The percentage of newly formed mullite and residual quartz content are inversely correlated to the quantity of amorphous phase (glass generated by melting of feldspars and illite) in the fired bodies. Fig. 5 evidences that increasing the amorphous phase content, the percentage of quartz and mullite decreases. The correlation between quartz and amorphous phase is less evident, because it is masked by the content of quartz in the unfired mixtures. As previously stated, quartz is unstable in the alkaline melt and tends to decompose whereas mullite formation is inhibited, because of the depletion of Al and Si ingested in the alkaline glass. Quartz fraction ranges between 16.3 wt.% (C, with 63.1 wt.% of amorphous) and 10.6 wt.% (G, 82.0 wt.% of glass); mullite ranges from 1.9 wt.% (H, 81.1 wt.% of glass) to 11.3 wt.% (C).

Table 4

Linear shrinkage, water absorption percentage values and Rietveld quantitative phase analysis (wt.%), of the tiles fired at 1200 °C

	A	B	C	D	E	F	G	H
Linear shrinkage (%)	5.82	5.14	6.08	5.10	6.01	5.96	3.96	4.82
Water absorption (%)	2.36	1.70	0.00	0.00	0.00	0.00	0.00	0.00
Quartz	13.0(1)	15.5(1)	16.3(1)	15.6(1)	15.4(1)	14.5(1)	10.6(2)	12.2(2)
Mullite	5.7(3)	5.1(3)	11.3(3)	7.5(3)	7.1(3)	5.8(3)	2.2(4)	1.9(4)
Plagioclase	5.3(2)	3.9(1)	9.3(2)	5.2(2)	3.1(2)	3.8(3)	3.9(4)	3.7(4)
K-feldspar	0.2(1)	0.2(1)	–	0.6(2)	1.0(3)	0.8(3)	1.3(4)	1.1(4)
Amorphous	75.8(7)	75.3(6)	63.1(6)	71.1(8)	73.4(9)	75.1(1.0)	82.0(1.4)	81.1(1.4)

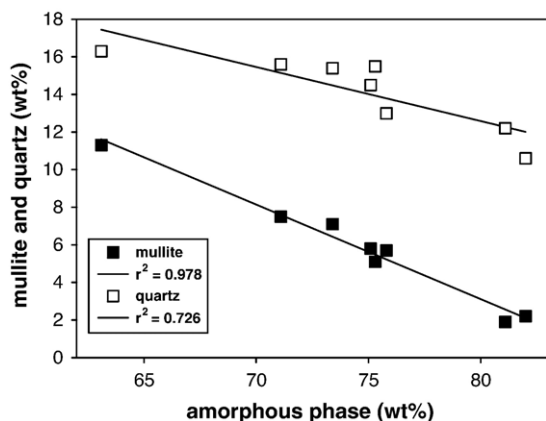


Fig. 5. Correlation between amorphous phase and mullite and quartz formed after firing in the fired ceramic mixtures.

Water absorption and linear shrinkage measured on the bodies fired at 1200 °C are shown in Table 4. Water absorption is zero for samples C–H whereas it is larger than zero in the mixtures A and B which contain the highly refractory kaolinitic clay. The value measured in A (2.36%) is larger since the content of kaolinite and the ratio kaolinite/quartz was higher in C1 with respect to C2. The SEM images reported in Fig. 6 well exhibit the difference in microstructure of the refractory mixtures (mixture A in 6A) and the fluxing ones (mixture H in 6B). In fact, Fig. 6A shows open porosity, apparently no glass, and several crystals with shaped edges still present or newly formed. Oppositely, Fig. 6B depicts pores evenly distributed in the bulk with a small diameter (up to 15 μm) and no interconnected channels which explains the zero water absorption.

The firing curves of the eight investigated mixtures in the temperature range 1130–1220 °C are shown in Fig. 7 (water absorption) and Fig. 8 (linear shrinkage). The mixtures containing larger fractions of illite exhibit zero water absorption at lower temperatures

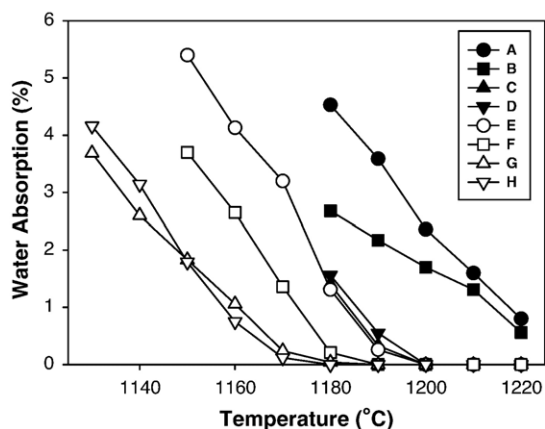


Fig. 7. Variation of the water absorption after firing in the range 1130–1220 °C.

with respect to the others. G and H have already vitrified at 1180 °C, C–F between 1190 and 1200 °C whereas A and B are just sintered at 1220 °C. Consequently, the linear shrinkage ranges between 3.62% (G) and 6.08% (C). In general the curves show a steep increase followed by a plateau (indicative of the optimal firing temperature), and a slight decrease caused by the expansion and deformation of the ceramic bodies. The temperature at which the larger value is reached depends on the mineralogical and chemical content of the mixtures. Maximum values for G and H are measured at 1170 °C, whereas the temperature increases up to 1180 °C for F and 1200 °C for C, D and E. The behavior described above cannot be applied to A and B, which show a monotone increase of the linear shrinkage, due to sintering.

Table 5 reports the color parameters measured for the bodies fired at 1220 °C (mixtures A–F) or at 1200 °C (G and H). The determination of the color parameter indicates that A is the whitest body mixture, according to its large content of pure kaolinite. The measured  $L^*$

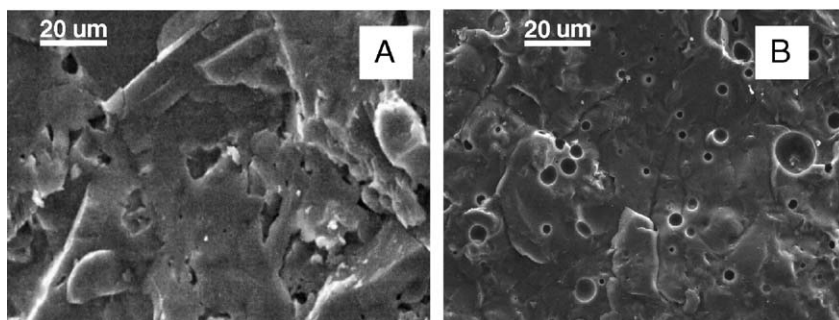


Fig. 6. SEM images of the bulk of the mixture A fired at 1200 °C (A) and mixture H fired at 1180 °C (B).

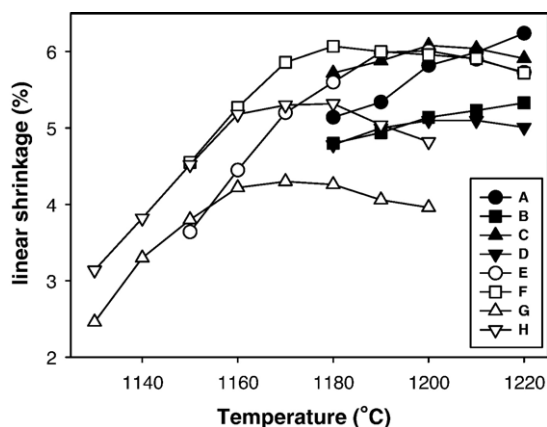


Fig. 8. Variation of the shrinkage after firing in the range 1130–1220 °C.

value is correlated with the iron content, higher this last and higher the  $L^*$  value (Fig. 9). G and H seem to be in disagreement with this trend because they are fired at a lower temperature (1200 °C instead of 1220 °C). In all the samples a positive value for  $a^*$  and  $b^*$  was measured, thus the color tends rather to red and yellow, than to green and blue. The shift towards the red tonality is connected to the conditions during firing, other than the iron amount. As a matter of fact,  $a^*$  ranges between 2 and 3 in samples A–D and increases up to 4.93 in E and F. G and H behave differently. Fe content is very low, but  $a^*$  values are the largest measured values (4.66 for G and 5.85 for H). This different behaviour could be explained by invoking a different atomic environment for iron in the structure of the crystalline phases. A twofold reason explains the enhanced dark-red color of the fired samples G and H: the presence of goethite in the starting raw materials and the low amount of newly formed mullite in the fired products. Iron is generally present in clay minerals which later in firing are responsible for the formation of mullite. In turn, mullite may host iron in the structure and thus inhibit the colouring of the body. In fact, the brownish color is determined by the presence of iron oxides eventually formed at expenses of Fe-hydroxides [like goethite,  $\alpha$ -FeO(OH)] following the reaction  $2\text{FeOOH} \rightarrow \text{Fe}_2\text{O}_3 + \text{H}_2\text{O}$ . Concerning iron in mullite, Schneider (1990)

Table 5  
Color parameters of samples fired at 1220 °C (A–F) and at 1200 °C (G and H)

	A	B	C	D	E	F	G	H
$L^*$	83.16	71.45	65.11	73.50	58.35	62.29	72.91	69.04
$a^*$	2.52	1.78	3.07	2.20	4.93	4.00	4.66	5.85
$b^*$	8.44	9.92	16.92	13.83	15.08	17.79	8.44	8.64

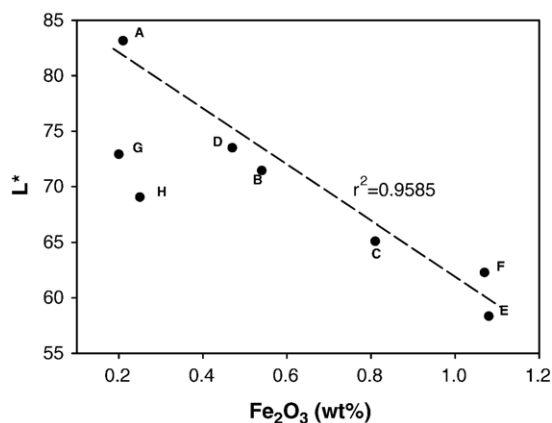


Fig. 9. Variation of the  $L^*$  color value as a function of the iron content in the ceramic mixture.

has shown that significant solubilities are only obtained with trivalent transition elements, such as Fe (III). Its solubility maximum value corresponds to 10–11 wt.%  $\text{Fe}_2\text{O}_3$  (Schneider and Rager, 1986).

In the mixtures prepared with the Hungarian clays, Fe is not part of the clay framework but is present as goethite phase which readily leads to the formation of hematite in firing with the consequence to make less iron available for mullite. In addition, as shown in Table 4, the percentage of newly formed mullite is very low in mixtures G and H, with respect to the other mixtures. Thus, a very minor quantity of Fe can be eventually host in the structure of mullite.

#### 4. Conclusions

As concluding remarks, the following aspects related to the presence of illite in ceramic mixtures for traditional ceramics can be summarized:

1. Concerning the technological parameters of the fired bodies, increasing illite content determines a larger percentage of glass phase and lower water absorption. We could expect linear shrinkage to increase with the increasing of illite content. On the contrary we observe a decreasing of that parameter due to pyroplastic deformation. In the case of kaolin, measured values of linear shrinkage and water absorption evidence the formation of a refractory amorphous phase and not a melt.
2. Increasing content of illite in the mixtures determines a decrease of mullite, cristobalite and quartz in the fired products. Free alumina and silica are depleted for the formation of the alkaline glass and quartz is unstable in the alkaline melt.



3. The mixtures with the Hungarian clays display the lowest melting spots because of the fluxing action of such clays.
4. Specific surface is mainly dependent upon illite content; the value is increased of about 30% using an illite-rich clay such as the Hungarian one with respect to a kaolinite-rich clay such as the Czech kaolin.
5. Illite has a twofold action in stoneware tiles mixtures. It gives plasticity and has a fluxing action.
6. The color of mixtures with Hungarian clays tends to be darker even if they contain a lower quantity of transition elements. This is due to the presence of goethite, which can be rapidly decomposed into hematite with temperature, and the low content of newly formed mullite, which could eventually host Fe in the structure.

#### Acknowledgements

The authors would like to thank Caolino Panciera S.p.A. (Italy) and Inter-Ili Engineering Office Co. Ltd. (Hungary) for providing the investigated raw materials studied. P. Pizzoli of the research laboratory of EmilCeramica S.p.A. and A. Tucci of the Centro Ceramico Bologna are greatly acknowledged for the technological measurements performed on raw materials and fired bodies. Because this manuscript is the outcome of a long-term project including sub-projects of degree thesis of P. Caliceti, G. Pietropaolo and E. Ori, we are indebted to them all.

#### References

- Aras, A., 2004. The change of phase composition in kaolinite- and illite-rich clay-based ceramic bodies. *Appl. Clay Sci.* 24, 257–269.
- Biffi, G., 1997. Il gres porcellanato: manuale di fabbricazione e tecniche di impiego. Faenza Editrice. In Italian.
- Ferrari, S., Gualtieri, A.F., Grathoff, G.H., Leoni, M., 2005. Model of structure disorder of illite: preliminary results. *Z. Kristallogr.* In press.
- Grim, R.E., Bray, R.H., Bradley, W.F., 1937. The mica in argillaceous sediments. *Am. Mineral.* 22, 813–829.
- Inoue, A., Kohyama, N., Kitagawa, R., Watanabe, T., 1987. Chemical and morphological evidence for the conversion of smectite to illite. *Clays Clay Miner.* 35, 111–120.
- Larson, A.C., Von Dreele, R.B., 1994. General Structure Analysis System (GSAS), Los Alamos National Laboratory, Document LAUR 86-748.
- Phelps, G.W., Harris, D.L., 1967. Specific surface and dry strength by methylene blue adsorption. *Am. Ceram. Soc. Bull.* 47, 1146–1150.
- Rieder, M., Cavazzini, G., D'Yakonov, Y.S., Frank-Kamenetskii, V.A., Gottardi, G., Guggenheim, S., Koval', P.V., Müller, G., Neiva, A. M.R., Radoslovich, E.W., Robert, J.L., Sassi, F.P., Takeda, H., Weiss, Z., Wones, D.R., 1998. Nomenclature of the micas. *Clays Clay Miner.* 46, 586–595.
- Rosenberg, P.E., 2002. The nature, formation, and stability of end-member illite: an hypothesis. *Am. Mineral.* 87, 103–107.
- Schneider, H., 1990. Transition metal distribution in mullite. *Ceram. Trans.* 6, 135–157.
- Schneider, H., Rager, H., 1986. Iron incorporation in mullite. *Ceram. Int.* 12, 117–125.
- Środoń, J., Eberl, D.D., 1984. Illite. *Mineral. Soc. Am. Rev. Mineral.* 13, 495–544.
- Young, R.A., 1993. *The Rietveld Method*. Oxford University Press.